

Supplementary Materials for **On-chip dual-comb source for spectroscopy**

Avik Dutt, Chaitanya Joshi, Xingchen Ji, Jaime Cardenas, Yoshitomo Okawachi, Kevin Luke,
Alexander L. Gaeta, Michal Lipson

Published 2 March 2018, *Sci. Adv.* **4**, e1701858 (2018)
DOI: 10.1126/sciadv.1701858

The PDF file includes:

- Details of soliton mode-locking using heaters
- Details of rf multiheterodyne spectroscopy
- Filtering
- Beat-note spacing
- Evolution of combs in the high-noise state
- Details of the experimental setup
- fig. S1. Detailed experimental setup.
- fig. S2. Heater response.
- fig. S3. Frequency comb filtered with a longpass filter.
- fig. S4. Quality factor of microrings.
- fig. S5. Optical spectra of combs in the high-noise state.
- fig. S6. Evolution of dual-comb beat note when the R1 comb is in the high-noise state.
- Legend for movie S1
- References (59–64)

Other Supplementary Material for this manuscript includes the following:
(available at advances.sciencemag.org/cgi/content/full/4/3/e1701858/DC1)

- movie S1 (.mp4 format). Beat-note evolution.

Supplementary Text

Details of soliton mode-locking using heaters

The difficulty in experimentally accessing the mode-locked regime of Kerr combs lies in the thermal shift of the resonance, which occurs on much slower timescales than the Kerr-nonlinear response. Tuning the rings into resonance with the pump at a slow speed typically leads to the formation of high-noise combs with multiple broad RF beat notes (23, 45, 59). This can be explained by the fact that the high noise state exists on the blue-detuned side of the resonance, where thermal shifts make the comb self-stable (60). Low-noise mode-locked states exist on the red-detuned side of the resonance, which by itself is thermally unstable. These mode-locked states, which correspond to temporal dissipative Kerr cavity solitons propagating in the microresonator, can be stably accessed by tuning into the red-detuned side of the resonance at an appropriate speed, so that the soliton state is reached when the cavity is close to its equilibrium temperature (45, 49). As mentioned in the main manuscript, we chose thermal tuning using integrated platinum microheaters to access the soliton mode-locked states because it allows us to tune at speeds of several tens of kHz, and because it enables us to use a fixed frequency low-noise laser as the pump.

We measured the response time of the heaters by applying a 4-mV peak-to-peak square wave voltage and monitoring the transmitted power through the bus waveguide as shown in fig. S2. We infer rise and fall times of 24 and 22 μs respectively from the exponential fits to the rising and falling edges of the transmitted optical power. The amplitude of the square wave voltage should be much smaller than the voltage required to tune across a ring resonance, to achieve a linear transduction of the voltage to the transmitted optical power and mitigate the effects of the nonlinearity of the Lorentzian response on the exponential fit. For good signal-to-noise ratio, the ring is operated near the maximum slope of the Lorentzian response for these measurements of the heater speed. Additionally, the power coupled to the bus waveguide is kept low ($\sim 70 \mu\text{W}$) to avoid significant thermal shift of the resonance. The 3-dB bandwidth of the heater response is 7 kHz, but the heaters can be operated at much higher speeds, albeit at a lower tuning efficiency.

Details of rf multiheterodyne spectroscopy

Filtering

Since the dual comb lines on the blue side of the pump are downmixed to the same RF frequency as the corresponding lines on the red side of the pump, we used short pass and long pass filters to separate the two halves of the dual comb spectrum. This enables one-to-one mapping of the comb lines to the RF beat notes. An example of a frequency comb filtered using a long pass filter is shown in fig. S3. In principle, an acousto-optic modulator (AOM) can be used to frequency shift a portion of the pump (28, 53, 61-64) and make the two resonators align to the two different wavelengths, which would alleviate the need for filtering the comb. It is worth noting that optical filtering is

routinely used to improve the SNR and prevent aliasing in dual comb spectroscopy (29, 53).

Beat-note spacing

The beat note spacing between the combs generated in rings R1 and R2 is determined by the difference in the radius of the two rings as well as the electrical power delivered to the microheaters. The rings were designed to have radii of 49.98 μm and 50.04 μm , which corresponds to an inherent nominal difference in their free spectral range (FSR) of 540 MHz. The heaters on R1 and R2 were driven with average powers of 94 mW and 30 mW respectively to make them resonant with the pump in tandem, which is responsible for a larger $\Delta f_{\text{rep}} = 1.12$ GHz.

It is important to note that $\Delta f_{\text{rep}} = 1.12$ GHz is larger than the cavity linewidth (~ 230 MHz for R1, 310 MHz for R2, see fig. S4), hence the comb lines generated in R1 do not resonantly couple into the longitudinal cavity modes of R2. Avoiding this coupling is essential to generate two separate combs with slightly different repetition rates, and prevent feeding of the second ring by the first comb. The rings are tuned such that the pump is the only wavelength that resonantly couples to both rings. Smaller beat note spacings $\Delta f_{\text{rep}} < 100$ MHz should be achievable using a parallel geometry instead of the cascaded or series geometry for the rings. In other words, the rings could be coupled to two separated bus waveguides, thus eliminating the possibility of the lines of the first comb feeding into the second ring. The loaded Q of the rings is 830,000 for R1 and 620,000 for R2. The rings are overcoupled, and the corresponding intrinsic Q is estimated to be $Q_{i,R1} \sim 5.7 \times 10^6$ and $Q_{i,R2} \sim 4.2 \times 10^6$ respectively. Significantly higher Q's up to 3.6×10^7 have recently been reported using improved fabrication techniques such as chemical mechanical planarisation, etching with reduced sidewall roughness, and multipass lithography (39). Silicon nitride microrings fabricated with these improved techniques would enable a smaller beat-note spacing even with a cascaded geometry since they would have an order of magnitude reduction in the resonance linewidths over the devices used in this work.

Evolution of combs in the high-noise state

It is essential to have both combs in the mode-locked state to observe the narrow beat notes shown in figs. 3 and 4 of the main manuscript. To prove this, we show the optical and RF spectra of non-modelocked combs in this section. Figure S5 depicts the mesa-shaped optical spectrum typically seen in combs in the high-noise state, as has been reported earlier (45, 49).

In fig. S6 we show the evolution of the first RF beat note at 8.6 GHz, using the device studied in Fig. 4 of the main manuscript. However, unlike what was reported in Fig. 4, the comb generated in R1 is not mode-locked, but in the high-noise state, while R2 is tuned into a resonance. The features observed on the blue-detuned side of the resonance are qualitatively similar to those observed when the R1 comb is mode-locked. On the other hand, the narrow high-SNR beat note is not observed on the red-detuned side of the

comb. This proves that the narrow intercomb beat note is only observed when both the combs are in the mode-locked state.

The linewidth of the beat note not only determines the relative coherence time of the two combs, but also limits the minimum beat note spacing that is permitted for them to be individually resolvable. The narrower the linewidth of the beat note, the higher the permissible compression ratio from the optical to the RF domain ($f_{\text{rep}}/\Delta f_{\text{rep}}$). It is thus important to operate both the combs in the mode-locked state.

Details of the experimental setup

We used a grade 3 RIO Orion laser, with a linewidth < 3 kHz. The phase noise is specified at $50 \mu\text{rad Hz}^{-1/2} \text{m}^{-1}$ at 10 Hz offset and $1.5 \mu\text{rad Hz}^{-1/2} \text{m}^{-1}$ at 10 kHz offset, normalized to a 1-m path difference. The output power was 21 mW. We attenuated the laser output by 10 dB before sending it to the EDFA. The EDFA had a noise figure of 4.8 dB (@-6 dBm input power) and was operated to output ~ 300 mW into the fiber.

The O/E element used in the measurement chain was a fast photodiode, New Focus 1014 InGaAs, with a bandwidth of 45 GHz, a rise time of 9 ps, a responsivity of 0.45 A/W and a noise-equivalent power of $45 \text{ pW Hz}^{-1/2}$. The photodiode signal was amplified using a three-stage broadband RF amplifier, Centellax OA4MVM3, with a bandwidth of 40 GHz, a gain of 27 dB and an rms timing jitter of 0.5 ps. The R1 and R2 combs are operated with pump power levels of approximately 105 mW and 130 mW in the bus waveguide respectively. The optical output powers of both the combs in the single-soliton state is ~ 12 mW excluding the pump.

Condensed-phase solids and liquids have broad absorption features, often spanning several tens of nm. The OSA has a resolution of 0.01 nm. The wavemeter (Advantest Q8326) has a higher absolute wavelength accuracy of 0.1 pm. The wavelength of the pump laser is precisely known to be 1561.413 nm, which was also verified by the wavemeter. These techniques combined with the equidistance of the RF beat notes within the resolution of our measurements (< 100 kHz) provide sufficient precision for calibrating the frequency/wavelength axis for condensed-phase spectroscopy and for studying comb-formation dynamics.

The generation of temporal dissipative Kerr solitons was observed to be highly repeatable in our experiments. Proper optimization of the parameters of the voltage ramp used to tune into resonance has allowed us to generate the same soliton mode-locked *single* frequency combs with each microresonator scan. For instance, see Fig. 5 in our recent work on thermally controlled soliton mode-locking Ref. (49). Dual comb generation is typically successful on each microheater scan, but occasionally requires multiple scans due to the effect of one ring's transmitted pump on the second ring. The chip's fabrication is also reproducible, as we used a well-documented fabrication process for the set of devices used in the experiment (36, 39). We consistently observe intrinsic quality factors in the several-million range using a standard fabrication process (36), and quality factors higher than 10 million using improved fabrication techniques (39). The

microheaters can compensate for fabrication deviations if needed. We fabricated microresonators with smaller and larger differences in ring radii (0.02 - 5 μm) and were able to reliably tune all the rings to the same pump laser in tandem. The achievable fabrication variation is well within the swept range.

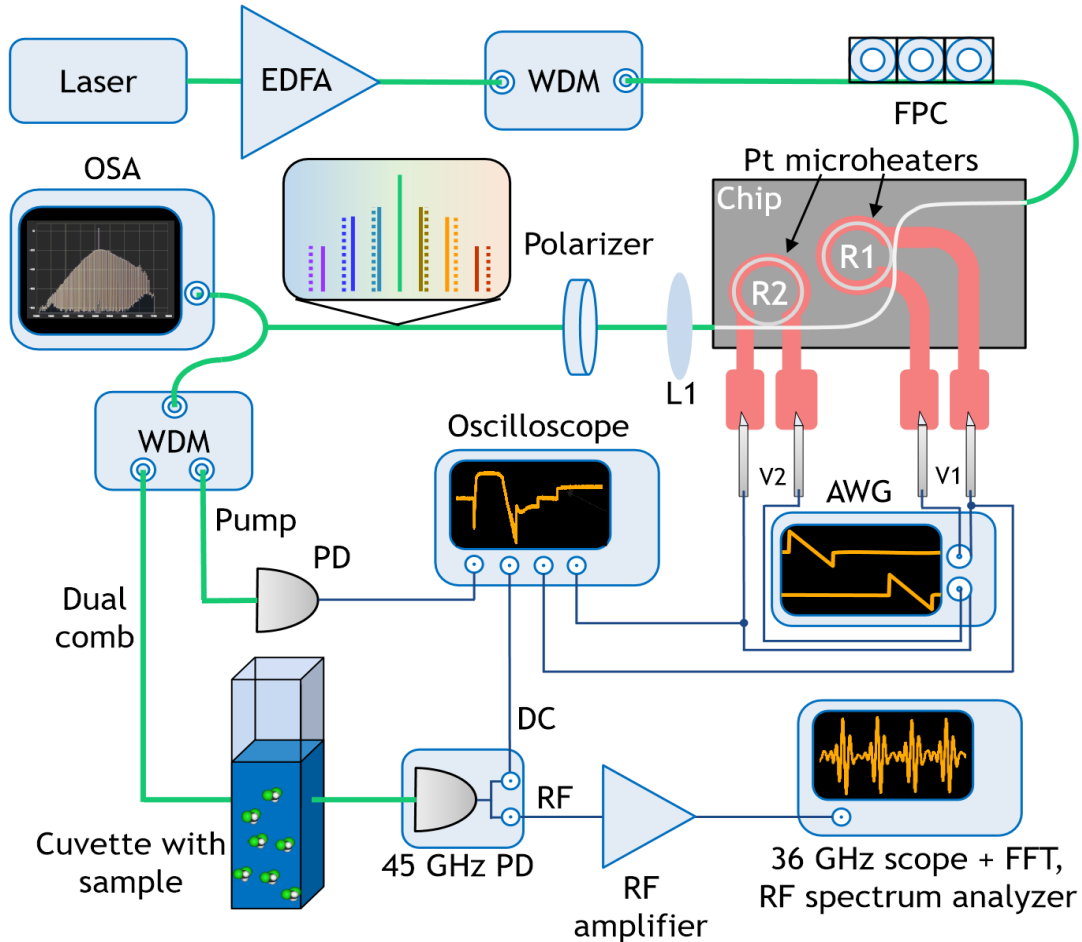


fig. S1. Detailed experimental setup. EDFA: erbium doped fiber amplifier. WDM: wavelength division multiplexing filter @ 1561.4 nm, 27.5 GHz 3-dB bandwidth. L1: 40x aspheric lens. FPC: fiber polarization controller. OSA: Optical spectrum analyzer. PD: photodiode. AWG: arbitrary waveform generator. V1 and V2 are voltages applied to the microheaters on rings R1 and R2.

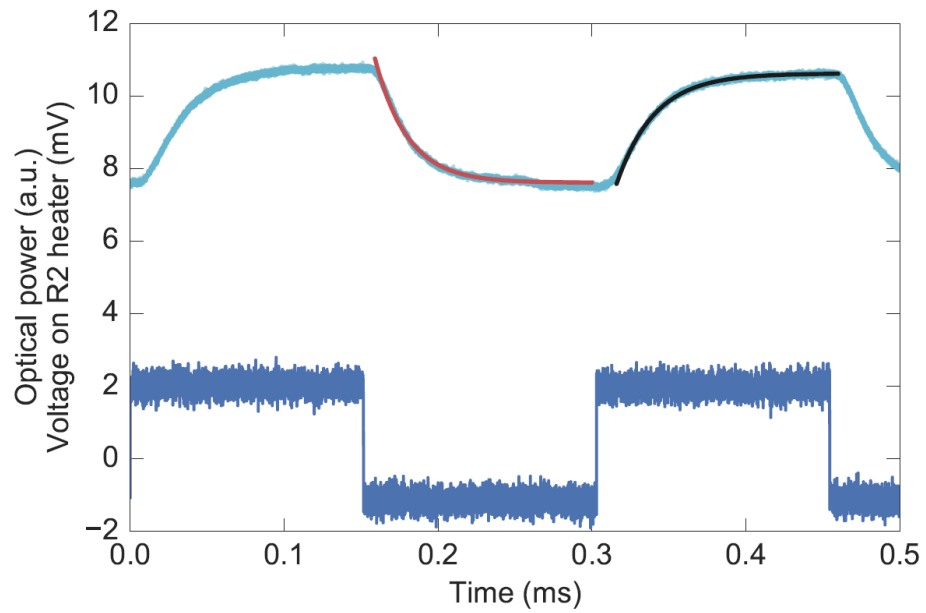


fig. S2. Heater response. A 4-mV peak-to-peak square wave modulation is applied to the heater on ring R1 at low optical powers in the bus waveguide. The dc offset of the applied voltage is tuned to bias the ring on one side of the resonance. An exponential fit to the optical transmitted power provides a rise time of 24 μs and a fall time of 22 μs .

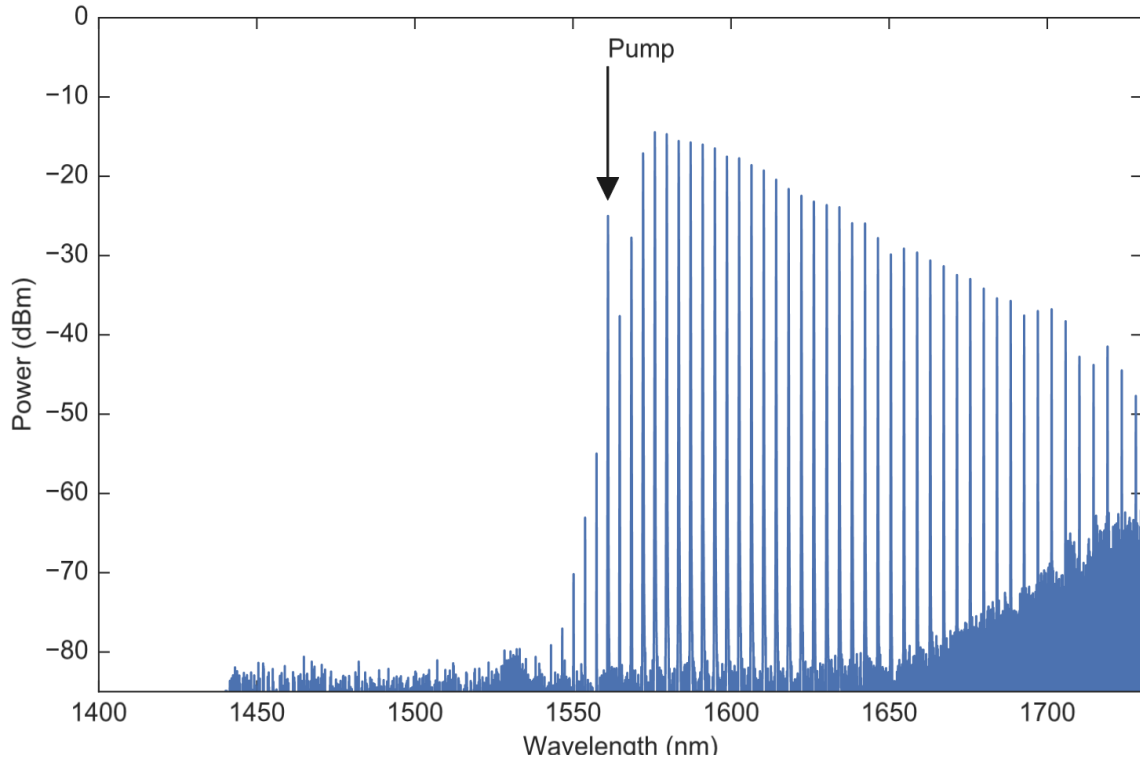


fig. S3. Frequency comb filtered with a longpass filter. An example of a comb filtered by an OD4 long pass filter with a cutoff wavelength at ~ 1560 nm.

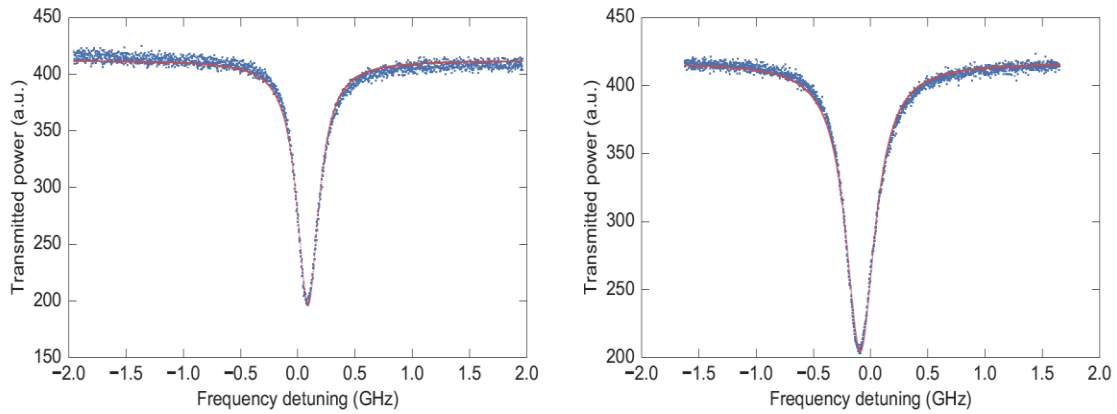


fig. S4. Quality factor of microrings. The full width at half maximum (FWHM) of the resonance estimated from the Lorentzian fit to the transmitted optical power is 230 MHz for R1 (left) and 310 MHz for R2 (right). This corresponds to loaded quality factors of 830,000 and 620,000 respectively. The power in the bus waveguide off resonance was approximately $20 \mu\text{W}$ for this measurement. Note that the FWHM is smaller than the beat note spacing of 1.12 GHz.

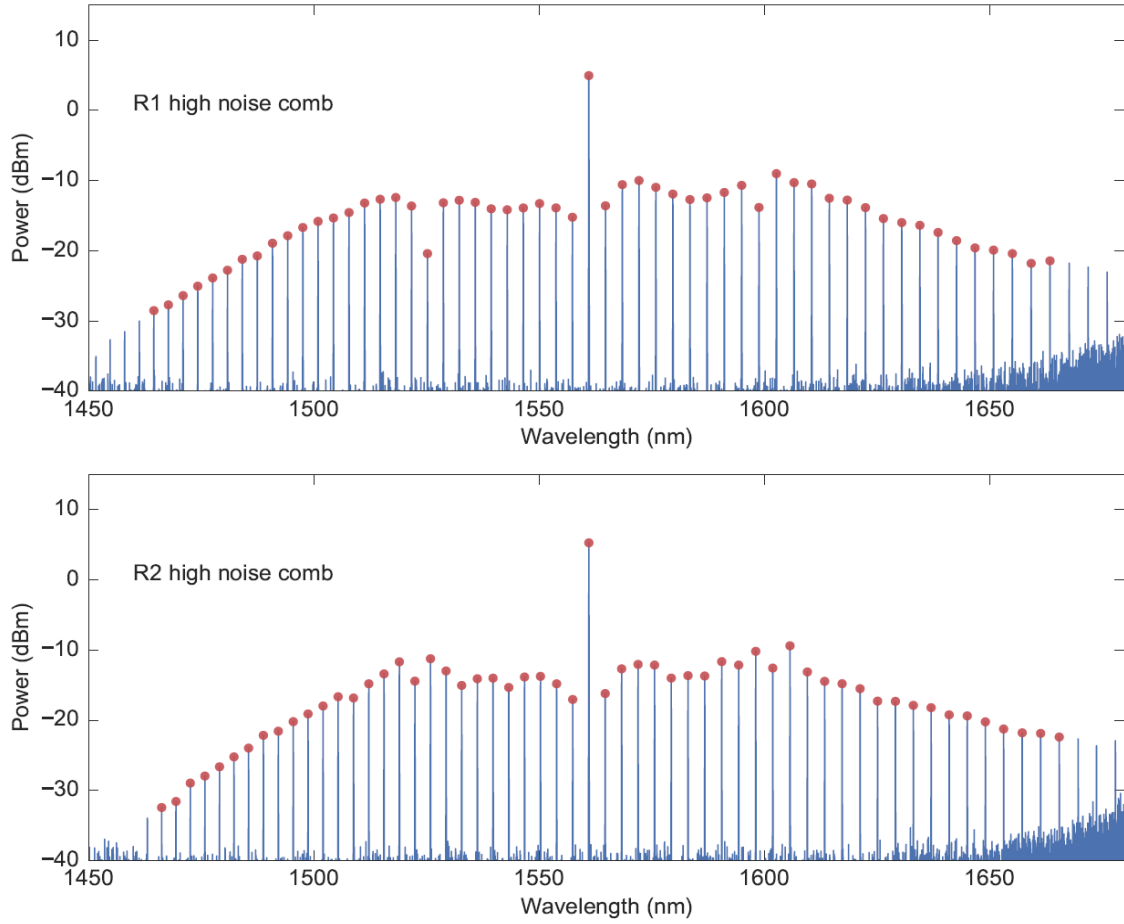


fig. S5. Optical spectra of combs in the high-noise state. The combs generated in R1 and R2 show a mesa-shaped spectrum. The device used here is the same as in Fig. 4, and had a $\Delta f_{\text{rep}} = 8.6$ GHz.

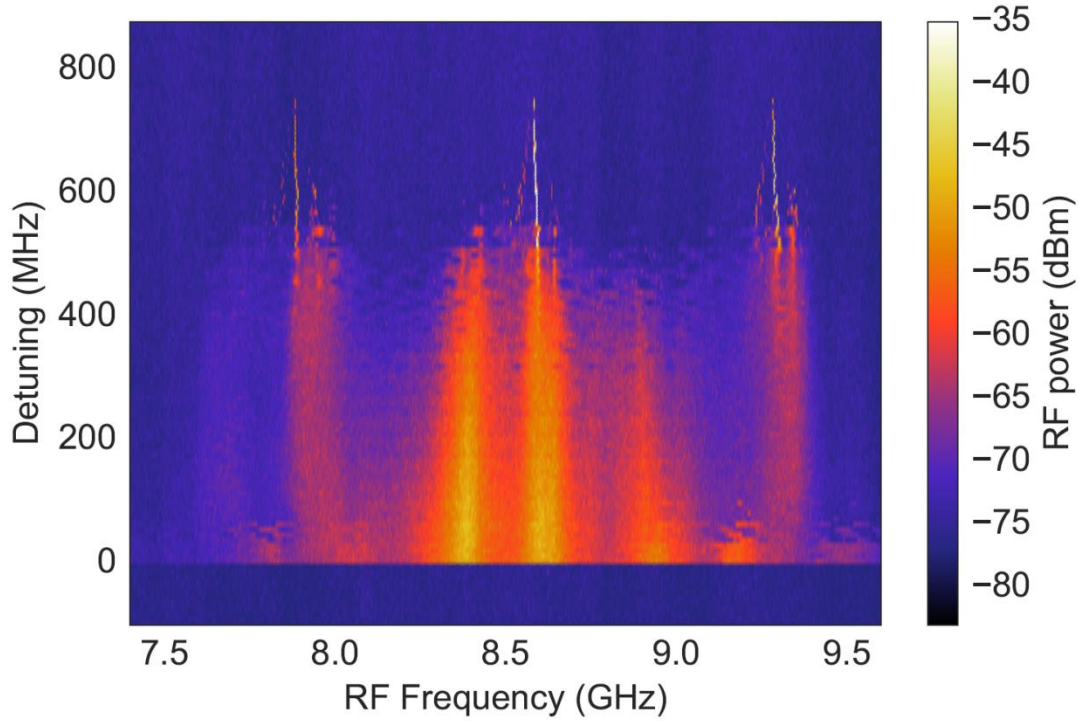


fig. S6. Evolution of dual-comb beat note when the R1 comb is in the high-noise state. Comparing with Fig. 4, we notice that the narrow high SNR beat note is absent on the red detuned side of the resonance. Hence, mode-locking both the combs is essential to observe the high SNR narrow beat note between the two combs of the dual comb. The device used here is the same as in Fig. 4, and had a $\Delta f_{\text{rep}} = 8.6$ GHz.

movie S1. Beat-note evolution. Movie showing the evolution of the RF beat-note at 8.6 GHz with detuning for the device and parameters described in Fig. 4 of the main manuscript text.